One-step Production of Polyelectrolyte Nanoparticles

Madeline Vauthier, Christophe Alexandre Serra

WILEY-VCH

DOI: 10.1002/ PI-20-0426

Article type: Research Paper

One-step Production of Polyelectrolyte Nanoparticles.

Madeline Vauthier, Christophe Alexandre Serra*

Dr. Vauthier, Prof. C.A. Serra
Université de Strasbourg, CNRS, Institut Charles Sadron UPR 22, F-67000 Strasbourg, France
*madeline.vauthier@ics-cnrs.unistra.fr

ABSTRACT.

Neutral polymeric nanoparticles have found many important applications in fields such as drug delivery, biosensing and environmental research. However, charged polymeric nanoparticles did not yet find such success mainly due to the multi-step and time-consuming conventional production route. Emulsification-evaporation method was described as a fast and reproducible way to obtain neutral polymeric nanosuspensions. We propose here, for the first time, to extend this method to the one-step production of negatively charged polymeric nanoparticles. In this purpose, we compared different processes, such as sonicator, shear mixer and elongational-flow reactor and mixer (µRMX) in order to produce polyelectrolyte nanoparticles (PNPs) of poly(styrene sulfonate). We found that only µRMX allowed the production of highly monodispersed PNPs. We also verified the decrease of nanoparticles' size (from 300 to 150 nm) and polydispersity index by increasing the emulsification's time and decreasing the polymer's molecular weight. Finally, we observed and explained the causes of an unusual behavior: the sudden increase of PNPs' size after a given emulsification time when using the elongational-flow reactor and mixer.

KEYWORDS. polyelectrolyte nanoparticles; emulsification-evaporation; elongational-flow, biocompatible polymer; dynamic light scattering; transmission electronic microscopy.

1. INTRODUCTION

Polyelectrolytes are polymers possessing many ionizable groups. The combination of polymeric and electrolyte behaviors gives them useful properties, such as drastically changing the properties of solutions and emulsions or interacting with ions and oppositely charged (macro)molecules. Polyelectrolytes could be classified as anionic, cationic or ampholytic, depending if the polymer carry negative, positive or both charges; they can also incorporate biological moieties (e.g. nucleic acids). Most polyelectrolytes are composed of the following synthetic polymers: poly(styrene sulfonic acid), poly(acrylic acid), poly(ethyleneimine).[1,2] Their assembly was well described in the literature, especially by G. Decher in 1997.[3] Indeed, polyelectrolytes can be deposited on surfaces in selectively permeable membranes[4–6]; used in solution as flocculants or dispersants[7,8] and for DNA studies[9] or on the external surface of particles.[10–12] In the literature, the study of polyelectrolytes microparticles, produced by droplet coalescence or by coating previously prepared inorganic microparticles for example, was well described (cytotoxicity, stability, binding)[10–13] but less examples of the production of polyelectrolytes nanoparticles (PNPs) could be found.[14–16] For instance, Shu *et al.* produced PNPs by mixing negatively and positively charged polymers by a dropping method under magnetic stirring. After two filtration-drying steps, the particles were redispersed and the resultant emulsion was stirred for 30 min to allow the formation of uniform nanoparticles.[15] However, it is sometimes hard to upscale the production of polyelectrolyte (nano)particles because they are conventionally elaborated in several steps: (i) the synthesis of polyelectrolyte, (ii) the formation of the organic or inorganic particle without polyelectrolyte and (iii) the deposition of alternatively charged polyelectrolytes onto the particle. Tackling with this point is part of

the present study. Moreover, previous works conducted on the elongational-flow reactor and mixer aimed at investigating effects of some process (pressure, number of cycles, geometry of the mixing elements) and composition parameters (amount of surfactant, volume fraction of the dispersed phase) on the droplet size for reference monomers (methyl acrylate and ethyl acrylate) and characteristics of subsequent polymeric nanoparticles obtained after UV-irradiations.[17-19] In brief, the use of PNPs in therapeutic delivery, biotechnology, magnetic separation or diagnostic imaging would allow to combine the advantages of inorganic charged particles (contrast agents, phases compatibilizers, electro-sensitivity) and the biocompatibility of polymers. So, we compared different emulsification-evaporation processes (sonication, shear mixing and elongational-flow micromixing) to demonstrate, for the first time, the possible one-step formation of polymeric charged nanoparticles from an already synthesized charged polymer.

2. MATERIALS AND METHODS

2.1. Materials

Poly(styrene sulfonate) PSS (Polymer Standards Service GmbH, counter-ion: Na^+) as a strong anionic polyelectrolyte, ethyl acetate (Sigma) and Pluronic® F-127 (triblock PEO–PPO–PEO copolymer of poly(ethylene oxide) (PEO) and poly(propylene oxide) (PPO), Sigma) as a non-ionic surfactant were used as received. The non-ionic surfactant, soluble in water, was chosen to avoid the complexation with PSS. Pluronic® F-127 stabilized the particles once ethyl acetate was evaporated. As previously published,[20] a low surfactant concentration lead to the production of big particles. Various PSS of different molecular weights (900; 6000; 55,000 and 70,000 g mol^{-1}) were used in this study.

The aqueous continuous phase (85v%) was composed of 15 g L^{-1} of surfactant solubilized in deionized water. The dispersed phase (15v%) was composed of PSS (1%) solubilized in ethyl acetate. Indeed, in previous studies,[19,21] our team proved that the polymer concentration and the continuous/dispersed phase (C/D) volume ratio influenced a lot the particles' size: smaller particles were produced by decreasing the polymer concentration (down to 1w%) and/or by increasing the continuous/dispersed volume phase ratio (up to 85/15).

2.2. Production of emulsions

Polymeric emulsions were first formed due to bubbles implosion with an ultrasonic device (Bandelin, SONOPULS UW 2200, 450W, f = 20 kHz) operating in pulsed mode at a given processing cycle (t_{on}/t_{total}). The continuous and dispersed phases were introduced in a plastic vial before being sonicated for a given time. A cooling ice bath was applied to maintain the temperature at 293 K (temperature measured with RS-232 Data Logger thermometer from Omega). At the end of the operation, the samples were left overnight in a fume hood to let the polymers' solvent evaporated resulting in the final obtention of a polymeric colloidal nanosuspension.

Then, the rotor-stator mixer (IKA®-Werke, Ultra-Turrax® T25 basic, 800 W) allowed the formation of emulsions by shearing the two phases, introduced in a plastic vial before being mixed for a given time at a given speed. A cooling ice bath was applied to maintain the temperature at 293 K. At the end of the operation, the samples were left overnight in a fume hood to let the dispersed phase's solvent evaporated.

Finally, the continuous phase and the dispersed phase were used as the raw material for the elongational-flow system. As illustrated in Scheme 1, the emulsification system was mainly assembled with two mid-pressure syringe pumps (Cetoni, neMESYS® Mid Pressure Module) working in opposite phase at the

same reciprocating flow rate (infuse following by withdraw of a syringe counted for 1 cycle), two 25 mL stainless steel syringes (Cetoni) and one PEEK tee (Valco Vici). The system was controlled by the supplier's software to precisely operate flow rate (30 $mL.min^{-1}$). Two of the three tee drilled cylindrical microchannels (diameter of 150 µm) were connected to the syringes with two PTFE tubes (1.06 mm ID x 1.68 mm OD). The third one was used to collect the emulsion at the end of the operation. Then, the samples were poured in a vial and left overnight in a fume hood to let the polymer's solvent evaporated.

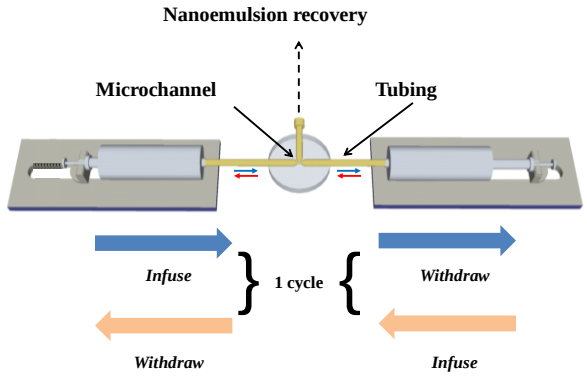

Scheme 1. Schematic illustration of the elongational-flow reactor and mixer.

After dialysis and freeze drying, the particles' yield was determined for sonicator (44%), for rotor-stator mixer (10%) and for elongational-flow reactor and mixer (72%) by the weight ratio between the particles after emulsion and the amount of polymer introduced in the device.

2.3. Characterization methods

Characterizations of the samples were realized one hour after the solvent's evaporation in three to five replicates. Three measurements were realized on each replicate.

2.3.1. Dynamic light scattering

The z-average diameter, size distribution and zeta potential of the nanoparticles (NPs) were assessed by dynamic light scattering (DLS) using a Nano ZetaSizer instrument (Malvern). The helium-neon laser (4 mW) was operated at 633 nm, the scatter angle was fixed at 173° and the sample temperature was maintained at 25°C. The polydispersity index of the particle size (PDI) was a measure of the broadness of the size distribution and it was commonly admitted that PDI values below 0.2 corresponded to monomodal distributions.[17, 22, 23] Analyses of nanoparticles' diameter were performed by pouring dropwise 0.02 mL of the nanosuspensions into 1 mL deionized water. Nine measurements were conducted for each returned value (three measurements on each of the three replicates), each measurement being an average of ten values calculated by ZetaSizer. All the zeta potential values were given at +/- 2mV due to the device precision.**2.3.2. Cryo-transmission electron microscopy**

To analyze the nanoparticles' morphology, cryo-transmission electron microscopy (cryo-TEM) has been chosen instead of TEM in order to fix the system and avoid NPs' degradation during the whole analysis procedure. A 5 µL drop of the nanosuspension was deposited onto a lacey-holey carbon film (Ted Pella) freshly glow discharged (Cordouan Technologies). The grid was rapidly frozen in liquid ethane cooled by liquid nitrogen in a home-made environment-controlled machine. The grids were mounted onto a Gatan 626 cryo-holder and observed in a Tecnai G2 (FEI-Eindhoven) operating at 200 kV and the images were taken with an Eagle 2k2k ssCCD camera (FEI- Eindhoven) under low dose conditions.

2.3.3. Viscometer

The viscosity of the different polymeric solutions was measured at 25°C by means of an Ostwald viscometer (CategorieI). This method was based on the determination of the time necessary to the solution to flow through a capillary. Each measurement was repeated four times and a mean value for the

flow time was taken. This time was then correlated to the kinematic viscosity $\nu = K (t-0)$. K was a constant related to the capillary (equal to 0.01 $mm^2 s^{-2}$ in our case), t was the average flow time (s) and 0 was the Hagenbach correction of time (s).

3. RESULTS AND DISCUSSION

In order to produce polyelectrolyte nanoparticles (PNPs) from a synthesized charged polymer, the continuous to dispersed phase volume ratio and the mixing parameters (MP) were fixed at reference values[18,19] and the emulsification time as well as the molar mass of the polyelectrolyte polymer were varied.

3.1. Influence of the processing parameters on the nanoparticle's properties

In a first part, the influence of the processing parameters on the PNPs' properties (size, PDI) was investigated. In this purpose, the PSS molecular weight M_w was fixed and equal to 70,000 $g.mol^{-1}$ and the continuous to dispersed phase volume (C/D) ratio was equal to 85/15. Emulsification times and mixing parameters (MP) employed are given in Table 1. Results are presented for the rotor-stator mixer, sonicator and elongational-flow reactor and mixer (μRMX) in Figure 1.

Table 1. Parameters used in this part in order to produce PSS (M_w = 70,000 g mol^{-1}) nanoparticles with three different emulsification devices.

Device	Emulsification times † (min)	Mixing parameter (MP)	C/D ratio
Rotor-stator mixer	5 to 40	17,500 rpm	85/15

Sonicator	5 to 40	50%	85/15
µRMX	20 to 120	30 mL min^{-1}	85/15

†These times were different because of the processes: after 40 min, the rotor-stator mixer and sonicator heated; before 20 min, the µRMX didn't allow the formation of nanoemulsions.

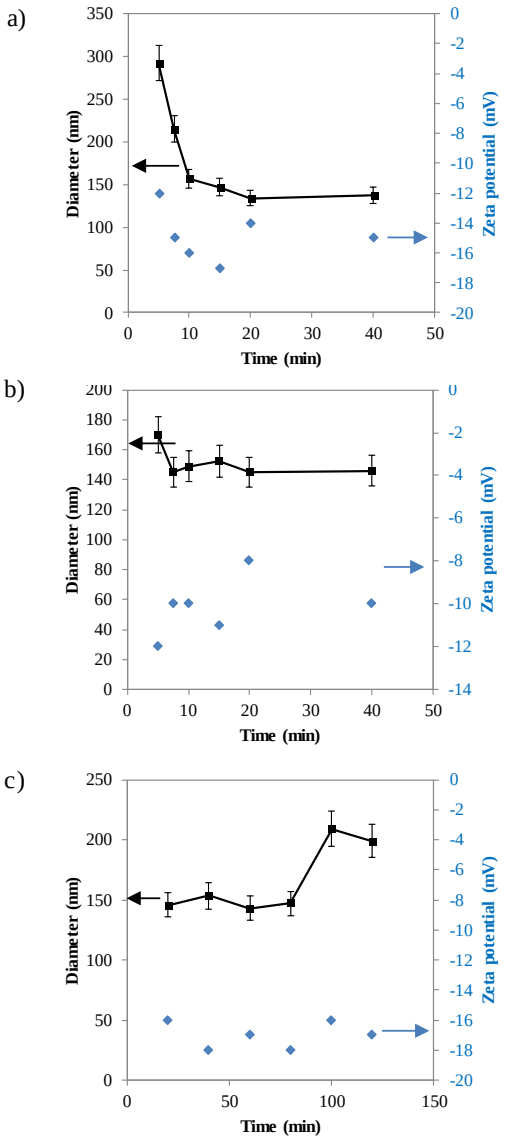

Figure 1. Evolution of PSS nanoparticles' size and zeta potential regarding to the emulsification time for a) rotor-stator mixer, b) sonicator and c) elongational-flow reactor and mixer (µRMX).

After a short emulsification time (around 5 minutes), there were huge size differences between the three devices: particles of 300 nm, 170 nm and 150 nm were produced with the shear mixer, the sonicator and the elongational-flow reactor and mixer respectively. This result, due to the different mechanisms of particle formation with these three devices, was coherent with previous study carried out by our team.[23] Indeed, particles were formed under different principles, by phase implosion with the sonicator, by shear forces with the rotor-stator mixer and thanks to a strong elongational flow (due to the reciprocating flow of the emulsion through an abrupt contraction induced by the microchannel) with the µRMX. More details about the formation of PNPs are given in Supporting Information (Scheme SI1). Interestingly, the lowest size achieved were 150 nm with all three devices. The possible formation of small particles was due to the presence of the charge on the polymer, as it was previously demonstrated by Reisch *et al*.[24] Indeed, the formation of negatively charged particles was proved by the zeta potential value, below -10 mV with all the three devices.

Increasing the emulsification time first decreased the PDI value from 0.71 ± 0.19 to 0.26 ± 0.03, from 0.37 ± 0.03 to 0.19 ± 0.02 and from 0.32 ± 0.05 to 0.18 ± 0.01 for the rotor-stator mixer, sonicator and µRMX respectively (Table SI1). The best results in terms of size monomodality were thus obtained with the sonicator and the elongational-flow reactor and mixer for a longer emulsification time. These differences in terms of size and PDI were confirmed by cryo-TEM micrographs (Figure 2).

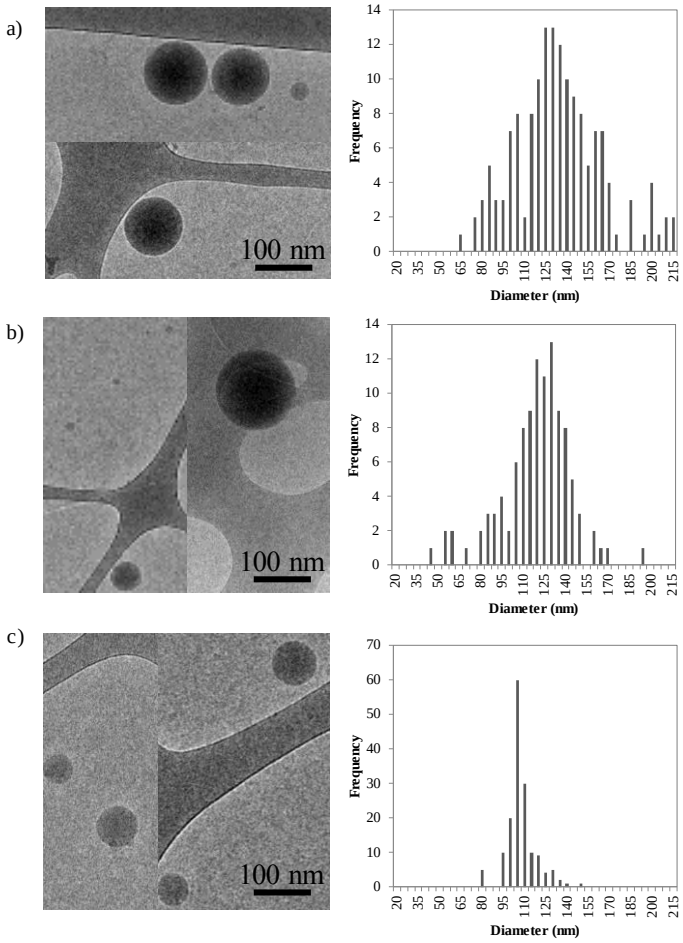

Figure 2. Cryo-TEM micrographs and statistical size analysis on 150 particles of PSS NPs elaborated in best conditions in terms of size and monomodality with a) rotor-stator mixer (20 min, 17500 rpm), b) sonicator (5 min, 50%) and c) elongational-flow reactor and mixer (60 min, 30 mL min^{-1}).

The PNPs' stability was also investigated by measuring their diameters over two months (Figure SI1). The results were process-depending since sonicator produced PNPs stable over one week before aggregation, rotor-stator mixer produced nanoparticles stable only one day and μRMX's PNPs were stable over one month.[25]

The elongational-flow reactor and mixer seemed to be the best device to obtain monodispersed and stable PNPs. However, an unusual and unexpected behavior was observed above 80 minutes of emulsification time: the PNPs' diameter increased drastically past this threshold time (Figure 1.c). This result could not be due to a process artefact because each experiment was carried out at least nine times. Since PSS is quite hydrophilic, this result might be interpreted by the penetration of water inside the particles or by a too long emulsification time which led to bigger particles due to extreme chain repulsion.

3.2. Influence of the polymers' chain length on the nanoparticle's size

In order to confirm previous assumptions, the influence of the polymer's chain length, *i.e.* the molecular weight M_w, on the PNPs' properties was studied for the elongational-flow reactor and mixer (Figure 3.a).

a)

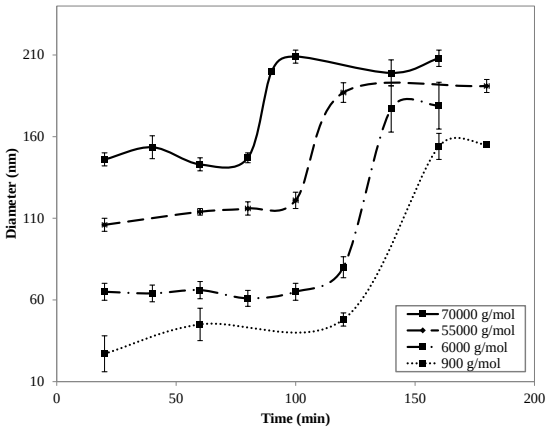

b)

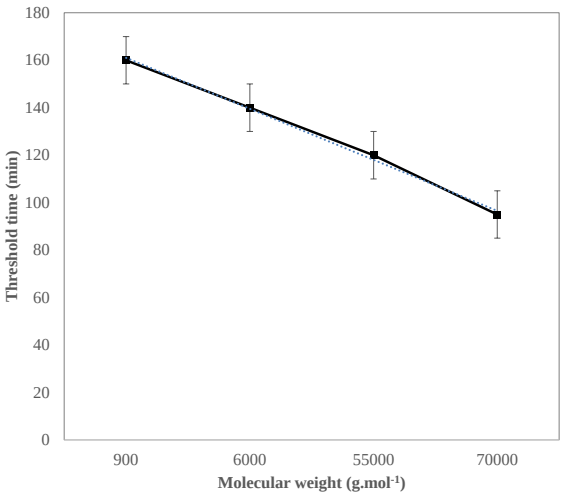

Figure 3. a) Effect of PSS molecular weight on the evolution of NPs sizes regarding to the emulsification time for the elongational-flow reactor and mixer (30 mL min^{-1}) and b) variation of the threshold time regarding to PSS molecular weight M_w. The equation of the fitting curve is *Threshold time* = $-22\ M_w + 183$ ($R^2 = 0.99$).

First, at low emulsification time, a plateau value was obtained for the diameter value. This value increased with the molecular weight and the polymer's viscosity. Indeed, the solution's dynamic viscosity (η) increases with the molecular weight (η = 12 mPas for 900 g mol^{-1} and η = 469 mPas for 70,000 g mol^{-1}; in agreement with the Mark–Houwink equation[26]), leading to higher particle's sizes. This behavior has already been investigated in the literature, for another chemical system[23] and was related to an increase in the critical capillary number, above which droplet scission may occur, which varies proportionally to the solution viscosity.

All the PSS had the same density of charge on their chains and, due to the formulation procedure, the polyelectrolytes had the same mass concentration in the emulsion. Chain repulsion should thus be the same for all polymers. However, the earlier size increase of particles of high-molecular weight might be

due to a small effect of electrostatic repulsion caused by the mobility of long ionic chains (rearrangement of polymer chains) at the interface between nanodroplets and the aqueous phase. Therefore, chain repulsion cannot explain by itself the different threshold times and increases of diameter observed.

However, since mass concentrations were the same, volume concentrations were different due to molecular weights. So, particles produced with a lower M_w were probably more compact, *i.e.* composed of more chains, than the one produced with a larger M_w.[27] This difference of chain compactness may lead to various osmotic pressure generated across the particles surface (more chains present, in the case of lower M_w, lead to a greater osmotic pressure), leading to different water penetration rates inside the PNPs, explaining why highly compacted PNPs swelled up more than less compact PNPs. Indeed, water penetration was probably favorized for small PNPs since it was easier to disentangle their chains. This various water penetration rates inside the PNPs also explained why highly compressed PNPs swelled up later than less compressed PNPs, *i.e.* those made from higher PSS molecular weights. Indeed, it was observed that the lower the molecular weight, the later the PNPs diameter increased: the diameter of PSS at 900 g mol^{-1} increased around 160 min, after 140 min for PSS at 6000 g mol^{-1}, after 120 min for PSS at 55,000 g mol^{-1} and around 90 min for PSS at 70,000 g mol^{-1}. It is noteworthy that this behavior satisfied a linear law (Figure 3.b) with a coefficient of determination R^2 equal to 0.99. Thus, it is possible to predict the threshold time only by knowing the PSS molecular weight M_w. It should be pointed out that the diameter difference before and after the threshold time decreased when the PSS chain length increases, which is also supported by the different swelling rates.

Finally, PNPs were stable regarding to chain repulsion and with the elongational-flow reactor and mixer, PNPs' diameter always increased at a given time, after the threshold time, mainly due to polymer

swelling. One could thus predict and control when this threshold time occurred in order to adapt the process conditions to obtain the desired PNPs size.

4. CONCLUSION

To conclude, three different devices (sonicator, rotor-stator mixer and elongational-flow reactor and mixer) were first used to produce nanosuspensions from negatively charged polyelectrolytes. The nanoparticles yield was 44% for sonicator, 10% for rotor-stator mixer and 72% for elongational-flow reactor and mixer. Various sizes and PDIs were obtained depending on the process. Indeed, the sonicator allowed the formation of monomodal nanosuspensions with particles' diameter lower than 200 nm; larger particles (ranging from 120 nm to 350 nm) with higher size dispersion were obtained with the shear mixer and monodispersed nanosuspensions of 150-200 nm were produced with the elongational-flow reactor and mixer. These sizes were smaller than the one presented in the literature.[28,29] Moreover, the elongational-flow reactor and mixer was the only one showing an unusual but yet interesting size behavior: the increase of PNPs' diameter after a given emulsification time (threshold time), due to water permeation inside polyelectrolyte nanoparticles.

This work allowed the controlled one-step production of monodispersed polyelectrolyte nanoparticles which size can be tuned just by varying process parameters. It will then be possible to continuously produce them, in order to reach industrial quantities for biomedical or drug delivery-related applications for example. Indeed, poly(styrene sulfonate) is biocompatible and sensitive to salt concentration.

ACKNOWLEDGMENTS

The authors would like to thank Mélanie Legros and Marc Schmutz for the access to the ICS characterization and electronic microscopy platforms respectively. Olivier Felix and Gero Decher are also thanked for their help.

Received: ((will be filled in by the editorial staff))
Revised: ((will be filled in by the editorial staff))
Published online: ((will be filled in by the editorial staff))

REFERENCES

(1) Rubinstein, M.; Papoian, G. *Soft Matter* **2012**, *8*, 9265–9267.
(2) Lyu, X.; Clark, B.; Peterson, A.M. *J. Pol. Sci. Part B* **2017**, *55* (8), 684-691.
(3) Decher, G. *Science* **1997**, *277* (5330), 1232–1237.
(4) Lvov, Y.; Haas, H.; Decher, G.; Moehwald, H.; Mikhailov, A.; Mtchedlishvily, B.; Morgunova, E.; Vainshtein, B. *Langmuir* **1994**, *10* (11), 4232–4236.
(5) Harris, J. J.; Stair, J. L.; Bruening, M. L. *Chem. Mater.* **2000**, *12* (7), 1941–1946.
(6) Schönhoff, M. *Current Opinion in Colloid & Interface Science* **2003**, *8* (1), 86–95.
(7) Mihai, M.; Ghiorghita, C. A.; Stoica, I.; Nita, L.; Popescu, I.; Fundueanu, Ghe. *Express Polym. Lett.* **2011**, *5* (6), 506–515.
(8) Zheng, X.; Luo, H.; Cao, W. *Polym. Int.* **2000**, *49* (11), 150-1504.
(9) Hsu, H.-P.; Lee, E. *Electrochemistry Communications* **2012**, *15* (1), 59–62.
(10) Hu, H.-Y.; Dou, X.-R.; Jiang, Z.-L.; Tang, J.-H.; Xie, L.; Xie, H.-P. *J Pharm Anal* **2012**, *2* (4), 293–297.
(11) Walker, H. W.; Grant, S. B. *Journal of Colloid and Interface Science* **1996**, *179* (2), 552–560.
(12) Sharma, A.; Tan, S. N.; Walz, J. Y. *Journal of Colloid and Interface Science* **1997**, *190* (2), 392–407.
(13) Weiss, L.; Zeigel, R. *Journal of Cellular Physiology* **1971**, *77* (2), 179–185.
(14) Zhang, S.; Yang, W.; Niu, Y.; Li, Y.; Zhang, M.; Sun, C. *Anal Bioanal Chem* **2006**, *384* (3), 736–741.
(15) Shu, S.; Zhang, X.; Teng, D.; Wang, Z.; Li, C. *Carbohydrate Research* **2009**, *344* (10), 1197–1204.
(16) Zaitsev, S.; Cartier, R.; Vyborov, O.; Sukhorukov, G.; Paulke, B.-R.; Haberland, A.; Parfyonova, Y.; Tkachuk, V.; Böttger, M. *Pharm Res* **2004**, *21* (9), 1656–1661.
(17) Ding, S.; Anton, N.; Vandamme, T. F.; Serra, C. A. *Expert Opinion on Drug Delivery* **2016**, *13* (10), 1447–1460.
(18) Souilem, I.; Muller, R.; Holl, Y.; Bouquey, M.; Serra, C. A.; Vandamme, T.; Anton, N. A Novel. *Chemical Engineering & Technology* **2012**, *35* (9), 1692–1698.
(19) Yu, W.; Serra, C. A.; Khan, I. U.; Ding, S.; Gomez, R. I.; Bouquey, M.; Muller, R. *Macromol. React. Eng.* **2017**, *11* (1), 1600024.
(20) Luque-Michel, E.; Sebastian, V.; 2 , Larrea, A.; Marquina, C.; Blanco-Prieto, M. J. *Eur J Pharm Biopharm.* **2019**, *145*, 65-75.
(21) Bally, F.; Garg, D.K.; Serra, C. A.; Hoarau, Y.; Anton, N.; Brochon, C.; Parida, D.; Vandamme, T.; Hadziioannou, G. *Polymer* **2012**, *53* (22), 5045-5051.

(22) Masarudin, M. J.; Cutts, S. M.; Evison, B. J.; Phillips, D. R.; Pigram, P. J. *Nanotechnol Sci Appl* **2015**, *8*, 67–80.
(23) Anton, N.; Bally, F.; Serra, C. A.; Ali, A.; Arntz, Y.; Mely, Y.; Zhao, M.; Marchioni, E.; Jakhmola, A.; Vandamme, T. F. A *Soft Matter* **2012**, *8* (41), 10628.
(24) Reisch, A.; Runser, A.; Arntz, Y.; Mély, Y.; Klymchenko, A. S. *ACS Nano* **2015**, *9* (5), 5104–5116.
(25) Grace, H.P. *Chemical Engineering Communications* **1982**, *14* (3-6), 225-277.
(26) Voeks, J. F. *Journal of Polymer Science.* **1959**, *36* (130), 333–339.
(27) Strobl, G. *Springer*. **2007**, 15-67.
(28) Choi, W. S.; Koo, H. Y.; Huck, W. T. S. *J. Mater. Chem.* **2007**, *17* (47), 4943–4946.
(29) Schatz, C.; Bionaz, A.; Lucas, J.-M.; Pichot, C.; Viton, C.; Domard, A.; Delair, T. *Biomacromolecules* **2005**, *6* (3), 1642–1647.